UDK 903'12/'15(4/5)"633/634":575.17; 903'12/'15(4/5)"633/634":574.91
Documenta Praehistorica XXXIV (2007)

A Pan-European model of the Neolithic

Kate Davison[1], Pavel M. Dolukhanov[2], Graeme R. Sarson[1], Anvar Shukurov[1] and Ganna I. Zaitseva[3]

1 *School of Mathematics and Statistics, University of Newcastle upon Tyne, NE1 7RU, U.K.*
kate.davison@ncl.ac.uk; g.r.sarson@ncl.ac.uk; anvar.shukurov@ncl.ac.uk
2 *School of Historical Studies, University of Newcastle upon Tyne, NE1 7RU, U.K.*
pavel.dolukhanov@ncl.ac.uk
3 *Institute for the History of Material Culture, Russian Academy of Sciences, St. Petersburg, Russia*

ABSTRACT – *We present a mathematical model, based on a compilation of radiocarbon dates, of the transition to the Neolithic, from about 7000 to 4000 BC in Europe. With the arrival of the Neolithic, hunting and food gathering gave way to agriculture and stock breeding in many parts of Europe; pottery-making spread into even broader areas. We use a population dynamics model to suggest the presence of two waves of advance, one from the Near East, and another through Eastern Europe. Thus, we provide a quantitative framework in which a unified interpretation of the Western and Eastern Neolithic can be developed.*

IZVLEČEK – *Predstavljamo matematični model, ki temelji na kompilaciji radiokarbonskih datumov med 7000 in 4000 BC. Ti datumi so v Evropi povezani s prehodom v neolitik, ko sta poljedelstvo in živinoreja v mnogih regijah zamenjala lov in nabiralništvo; lončarstvo pa se je širilo še dlje. S pomočjo modela populacijske dinamike predstavljamo dva vala napredovanja, enega iz Bližnjega Vzhoda in drugega preko Vzhodne Evrope. Z njim zagotavljamo kvantitavni okvir, v katerem lahko razvijamo enovito interpretacijo 'zahodnega' in 'vzhodnega' neolitika.*

KEY WORDS – *Neolithic; population dynamics; radiocarbon dates; archaeology; mathematical modelling*

Introduction

The transition to the Neolithic was a crucial period in the development of Eurasian societies, defining to a large extent their subsequent evolution. The introduction of agro-pastoral farming, which originated in the Near East about 12 000 years ago and then spread throughout Europe, is usually considered to be a key feature of this transition (*Zvelebil 1996*). Yet the Neolithic was not a simple, single-faceted phenomenon. In his early definition of the Neolithic, Sir John Lubbock (*1865*) specified its main characteristics to be the growing of crops, the taming of animals, the use of polished stone and bone tools, and pottery-making.

Ceramic pottery is one of the defining characteristics of the Neolithic. It is true that there are examples of early farming communities apparently not involved in pottery-making. For example, aceramic Neolithic cultures have been identified in the Levant, Upper Mesopotamia, Anatolia (9800–7500 BC) and also in the Peloponnese (7000–6500 BC) and Thessaly Plain (7300–6300 BC). (All BC dates supplied are radiocarbon dates calibrated using OxCal v3.10 (*Bronk Ramsey 2001*) with calibration curve intcal04.14c.) Wheat, barley and legumes were cultivated at those sites; permanent houses with stone foundations were used. There is no widespread evidence of pottery (*Perlès 2001*) but recent excavations have revealed the occurrence of pottery in Thessaly, albeit in small quantities (*J. K. Kozłowski, personal communication 27/03/2007*). In contrast, the Neolithic in North-Eastern boreal Europe is identified with a sedentary

(or seasonally sedentary) settlement pattern, social hierarchy and sophisticated symbolic expression, the use of polished stone and bone tools, large-scale manufacture of ceramic ware, but not with agriculture (*Oshibkina 1996*): the subsistence apparently remained based on foraging. This combination of attributes is characteristic of the 'boreal Neolithic'; of these, pottery is in practice the most easily identifiable.

In the present paper we attempt to develop a unified framework describing the spread of both the 'agro-pastoral' and 'boreal' Neolithic. Our quantitative model of the Neolithization is based on the large amount of relevant radiocarbon dates now available.

Selection of radiocarbon dates

The compilation of dates used in this study to model the spread of the Neolithic in Europe is available upon request from the authors; unlike all other similar studies known to us it includes dates from the East of Europe. We used data from Gkiasta et al. (*2003*), Shennan and Steele (*2000*), Thissen et al (*2006*) for Southern, Central and Western Europe (SCWE) and Dolukhanov et al. (*2005*), Timofeev et al. (*2004*) for Eastern Europe (EE). Our selection and treatment of the dates, described in this section, is motivated by our attempt to understand the spread of agriculture and pottery making throughout Europe.

Many archaeological sites considered have long series of radiocarbon dates: often with 3–10 dates, and occasionally with 30–50. Associated with each radiocarbon measurement is a laboratory error, which after calibration was converted into a calibration error σ_i. The laboratory error characterises the accuracy of the measurement of the sample radioactivity rather than the true age of the archaeological site (*Dolukhanov et al. 2005*) and, thus, is often unrepresentatively small, suggesting an accuracy of 30 years on occasion. Therefore, we estimated an empirical minimum error of radiocarbon age determination of the archaeological age and then used it when treating sites with multiple dates. A global minimum error of $\sigma_{min} = 160$ years is obtained from well explored, archaeologically homogeneous sites with a large number of tightly clustered dates. Such sites are: (1) Ilipinar, 65 dates, with the standard deviation $\sigma = 168$ years (and mean date 6870 BC); (2) Achilleion, 41 dates, $\sigma = 169$ years (mean 8682 BC); (3) Asikli Höyük, 47 dates, $\sigma = 156$ years (mean 7206 BC). Similar estimates are $\sigma_{min} = 100$ years for LBK sites and $\sigma_{min} = 130$ years for the Serteya site in North-Western Russia (*Dolukhanov et al. 2005*); the typical errors vary between different regions and periods but we apply $\sigma_{min} = 160$ years to all the data here.

For sites with multiple radiocarbon date determinations, the dates are treated and reduced to two (and rarely more) dates that are representative of the arrival of multiple Neolithic episodes to that location. For the vast majority of such sites, the radiocarbon dates available can be combined, as discussed below, to just two possible arrival dates. Examples of sites with multiple radiocarbon measurements are Ilipinar and Ivanovskoye-2 where, respectively, 65 and 21 dates have been published. Figures 1a and b indicate that for these sites the series of dates form very different distributions; different strategies are used to process these different types of date series as described below (see *Dolukhanov et al. 2005* for details). If a geographical location hosts only one radiocarbon measurement associated with the early Neolithic, then this is taken to be the most likely date for the arrival of the Neolithic. The uncertainty of this radiocarbon date is taken to be the maximum of the global minimum error discussed above and the calibrated date range obtained at the 99.7 % confidence level and then divided by six (to obtain an analogue of the 1σ error). There are numerous such sites in our collection, including Casabianca, Dachstein and Inchtuthil.

If only a few (less than 8) date measurements are available for a site and those dates all agree within the calibration error, we use their mean value and characterise its uncertainty with an error equal to the maximum of each of the calibrated measurement errors σ_i, the standard deviation of the dates involved $\sigma(t_i)$, $1 \le i \le n$, and the global minimum error introduced above:

$$\sigma = \max\left\{\sigma_i, \sigma\left(t_i\right), \sigma_{\min}\right\}, \qquad (1)$$

n is the total number of dates in the cluster. An example of such a site is Bademağaci, where we have 4 dates, all within 60 years of one another; Figure 1c shows the histogram of radiocarbon dates of this site. The typical calibration error of these dates is approximately 30 years, thus Eq. (1) yields σ_{min} as an uncertainty estimate. However, we apply a slightly different procedure for clusters of dates that do not agree within the calibration error.

For a series of dates that cluster in time but do not agree within the calibration error, we use different approaches depending on the number of dates available and their errors. Should the cluster contain less

than 8 dates, we take the mean of the dates (as in the previous case), as any more sophisticated statistical technique would be inappropriate for such a small sample; the error is taken as in Eq. (1). An example of such a site is Okranza Bolnica – Stara Zagora with 7 measurements, and Figure 1f shows that the dates are tightly clustered around the mean value.

If however, the date cluster is large (*i.e.* more than 8 dates, such as Ilipinar, shown in Fig. 1a), the χ^2 statistical test can be used to calculate the most likely date T of a coeval subsample as described in detail by Dolukhanov et al. (*2005*):

$$T = \frac{\sum_{i=1}^{n} t_i / \overline{\sigma}_i^2}{\sum_{i=1}^{n} 1 / \overline{\sigma}_i^2},$$

where $\overline{\sigma}_i = \max(\sigma_i, \sigma_{\min})$. The coeval subsample is obtained by calculating the statistic:

$$X^2 = \sum_{i=1}^{n} \frac{\left(t_i - T\right)^2}{\overline{\sigma}_i^2}$$

and comparing it with χ^2. If $X^2 \leq \chi^2_{n-1}$, the sample is coeval and the date T is the best representative of the sample. If $X^2 > \chi^2_{n-1}$, the sample is not necessarily coeval, and the dates that provide the largest contribution to X are discarded one by one until the criterion for a coeval sample is satisfied. This process is very similar to that implemented in the *R_Combine* function of OxCal (*Bronk Ramsey 2001*). However, OxCal's procedure first combines the uncalibrated dates into one single radiocarbon measurement and then calibrates it. Our approach on the other hand first uses the calibration scheme of OxCal and then combines the resulting calibrated dates to give *T*. Furthermore, our procedure adds the flexibility of identifying and discarding dates with the largest relative deviation from *T*. Within *R_Combine* the minimum error is not used in the calculation of X^2 but is rather only incorporated into the final uncertainty estimate. We feel that it is more appropriate to include the minimum uncertainty into the calculation from the outset. As a check, we combined several set of dates using both OxCal and our procedure, and the results agree within a few years in most cases where such agreement could be expected.

If a site has many radiocarbon determinations that do not cluster around a single date, a histogram of the dates is analyzed. If the data have a wide range and have no discernable peaks (*i.e.*, are approximately uniformly distributed in time), they may suggest prolonged Neolithic activity at the site, and we choose, as many other authors, the oldest date (or one of the oldest, if there are reasons to reject outliers) to identify the first appearance of the Neolithic. Examples of such sites are Mersin and Halula where there are 6 and 9 dates with a range of 550 and 1900 years, respectively, and no significant peaks (see Figs. 1d and 1e), here the oldest dates are 6950 and 8800 years BC and the associated errors are 217 and 167 years.

Apart from sites with either no significant peak or only one peak, there are sites whose radiocarbon dates have a multimodal structure which may indicate multiple waves of settlement passing through this location. Ivanovskoye-2 (with 21 dates) is a typical site in this category, and Figure 1b depicts two distinct peaks. In such cases multiple dates were attributed to the site, with the above methods applied to each peak independently. Admittedly our method of assigning an individual date to a specific peak could be inaccurate in some cases as appropriate stratigraphic and/or typological data are not invoked in our procedure. In future refinements to this technique we may consider fitting bimodal normal distributions to the data to avoid the rigid assignment of measurements to one peak or another. After selection and processing, the total number of dates in our compilation is 477. In our final selection, 30 sites have two arrival dates allocated and 4 sites have three arrival dates allocated, namely Berezovaya, Osipovka, Rakushechnyi Yar and Yerpin Pudas.

Modelling

The mechanisms of the spread of the Neolithic in Europe remain controversial. Gordon Childe (*1925*) advocated direct migration of the farming population; this idea was developed in the form of the demic expansion (wave of advance) model (*Ammerman and Cavalli-Sforza 1973*). The Neolithization was viewed as the spread of colonist farmers who overwhelmed the indigenous hunter-gatherers or converted them to the cultivation of domesticated cereals and the rearing of animal stock (*Price 2000*). An alternative approach views the Neolithization as an adoption of agriculture (or other attributes) by indigenous hunter-gatherers through the diffusion of cultural novelties by means of intermarriages, assimilation and borrowing (*Tilley 1994; Thomas 1996; Whittle 1996*). Recent genetic evidence seems to favour cultural transmission (*Haak et al. 2005*).

Irrespective of the particular mechanism of the spread of the Neolithic (or of its various signatu-

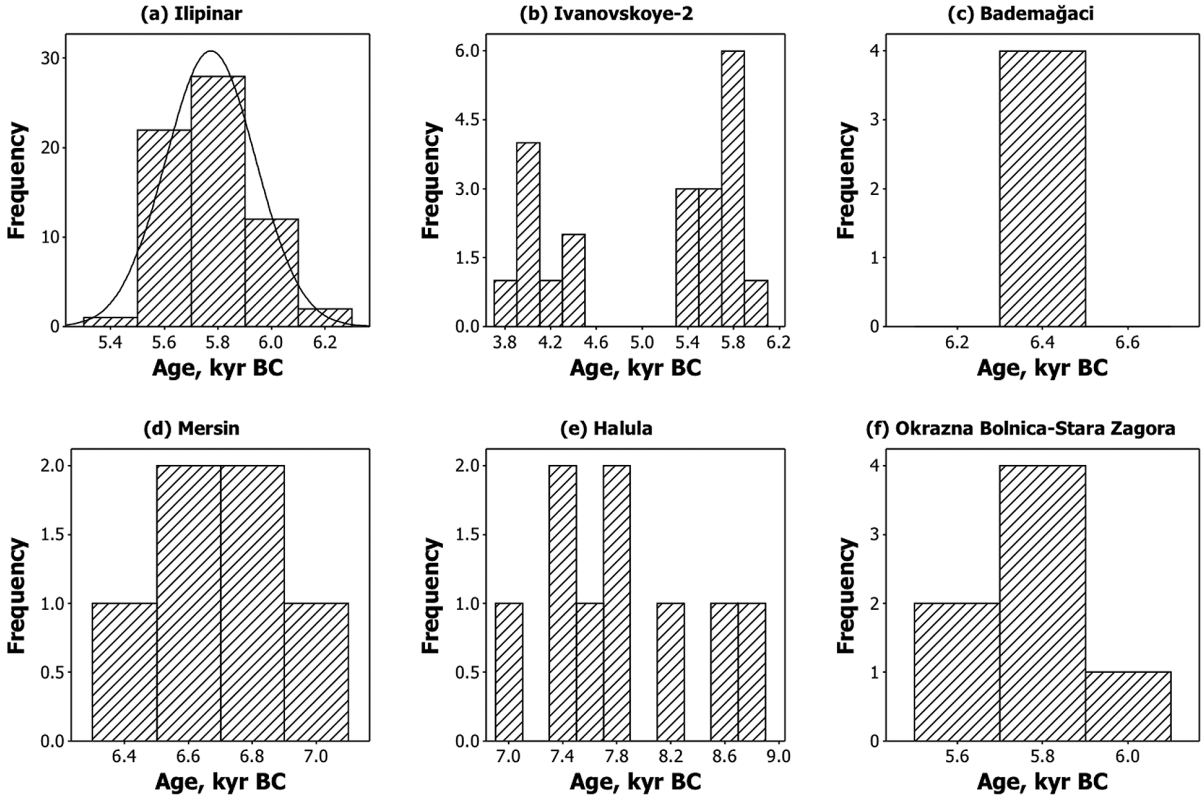

Fig. 1. Histograms of calibrated radiocarbon ages from archaeological sites in kyr BC, binned into 200 year intervals representing various temporal distributions. (a) The 65 dates from Ilipinar (40.47°N, 29.30°E) are approximately normally distributed, so the χ^2 criterion can be employed to calculate the age of this site as described by Dolukhanov et al (2005). The resulting Gaussian envelope is shown solid. (b) Ivanovskoye-2 (56.85°N, 39.03°E) has 21 dates showing a multimodal structure where each peak can be treated as above. (c) The 4 dates from Bademağaci (37.40°N, 30.48°E) combine into a single date when their errors are taken into account. (d) The 6 dates from Mersin (36.78°N, 34.60°E) are almost uniformly distributed in time, so the oldest date can be used as representative of the arrival of the Neolithic. (e) The 9 dates from Halula (36.40°N, 38.17°E) are treated as in (d). (f) The 7 dates from Okrazna Bolnica – Stara Zagora (42.43°N, 25.63°E) are not numerous enough to justify the application of the χ^2 test, but they form a tight cluster, so the mean date can be used for this site.

res), the underlying process can be considered as some sort of 'random walk', of either humans or ideas and technologies. Therefore, mathematical modelling of the spread (at suitably large scales in space and time) can arguably be based on a 'universal' equation (known as reaction-diffusion equation) with parameters chosen appropriately (*Cavalli-Sforza and Feldman 1981*). A salient feature of this equation is the development of a propagation front (where the population density, or any other relevant variable, is equal to a given constant value) which advances at a constant speed (*Murray 1993*) (in the approximation of a homogeneous, one-dimensional habitat). This mode of spread of incipient agriculture has been confirmed by radiocarbon dates (*Ammerman and Biagi 2003; Ammerman and Cavalli-Sforza 1971; 1973; 1984; Gkiasta et al. 2003; Pinhasi et al. 2005*). In Figure 2a we plot the distance from a putative source in the Near East versus the ^{14}C dates for early Neolithic sites in SCWE; the linear interdependence is consistent with a constant propagation speed. Due to the inhomogeneous nature of the landscape we would not expect to see a very tight correlation between distance from source and time of first arrival, since there are many geographical features that naturally cause barriers to travel (*e.g.* the Mediterranean Sea). It is also suggested in a previous work (*Davison et al. 2006*) that there are local variations in the propagation speed near major waterways; this again detracts from the constant rate of spread. In spite of this, the correlation coefficient is found to be –0.80; reassuringly high given the above complications. There is also a tail of older dates that originate in early Neolithic sites in the Near East, where a Neolithic tradition began and remained until it saturated the area and subsequently expanded across the landscape.

In contrast to earlier models, we include the 'boreal', East-European (EE) Neolithic sites, which we present

in the same format in Figure 2b. It is clear that the Eastern data are not all consistent with the idea of spread from a single source in the Near East. A correlation coefficient of –0.52 between the EE dates and distance to the Near East is sufficient evidence for that. Our modeling, discussed below, indicates that another wave of advance swept westward through Eastern Europe about 1500 years earlier than the conventional Near-Eastern one; we speculate that it may even have spread further to produce early ceramic sites in Western Europe (*e.g.* the La Hoguette and Roucadour groups).

Our population dynamics model, described in detail by (*Davison et al. 2006*), was refined for our present simulations. We thus solve the reaction-diffusion equation supplemented with an advection of speed **V**, arising from this anisotropic component of the random walk of individuals that underlies the large-scale diffusion (*Davison et al. 2006; Murray 1993*):

$$\frac{\partial N}{\partial T} + (\mathbf{V}\cdot\nabla)N = \gamma N\left(1-\frac{N}{K}\right) + \nabla\cdot(\nu\nabla N), \quad (2)$$

where N is the population density, γ is the intrinsic growth rate of the population, K is the carrying capacity, and ν is the diffusivity (mobility) of the population. We solve Eq. (2) numerically in two dimensions on a spherical surface with grid spacing of 1/12 degree (2–10 km, depending on latitude). All the variables in Eq. (2) can be functions of position and time, as described by Davison et al. (*2006*).

We consider two non-interacting populations, each modelled with Eq. (2), but with different values of the parameters **V**, γ, K and ν; the difference is intended to represent differences between subsistence strategies (farmers versus hunter-gatherers) and/or between demic and cultural diffusion.

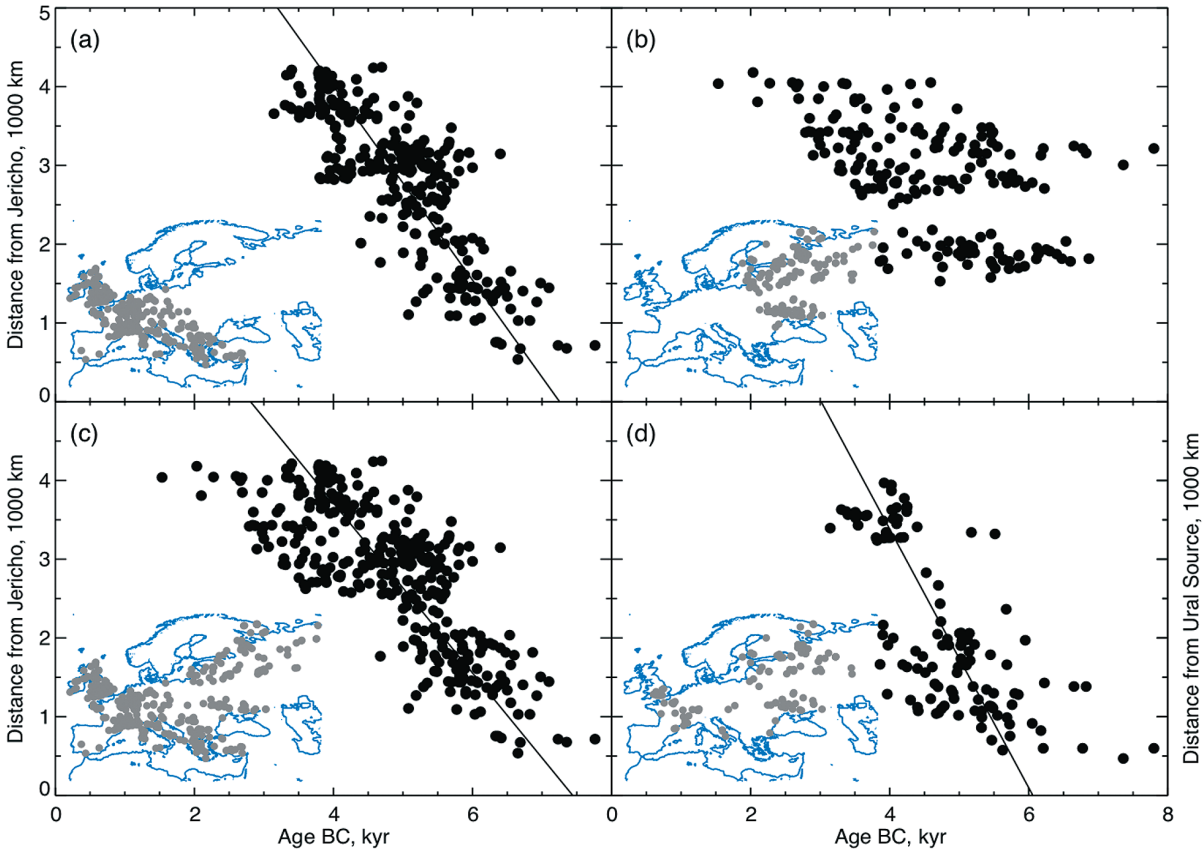

Fig. 2. Radiocarbon dates of early Neolithic sites versus the great-circle distance from the assumed source. Inset maps show the location of the sites plotted, and the straight lines correspond to spread at a constant speed given below. (a) Sites from Southern, Central and Western Europe (SCWE) with respect to a Near Eastern source (Jericho). The linear correlation (cross-correlation coefficient C = –0,80) suggests a mean speed of advance of U = 1.2 ± 0.1 km/year (2σ error). (b) Sites from Eastern Europe (EE) show very poor correlation with respect to the same Near-Eastern source (C = –0,52), so that straight-line fitting is not useful. (c) Sites attributed, using our two-source model, to the Near-Eastern source (note a significant number of EE sites clearly visible in the inset map) show a reasonable correlation (C = –0,77) and a mean speed U = 1.1 ± 0.1 km/year. (d) Sites attributed to the Eastern source (from both EE and SCWE) show a correlation similar to that of Panel (c) (C = –0,76), and a mean speed U = 1.7 ± 0.3 km/year.

We thus numerically solve two versions of Equation (2), one for each of two non-interacting populations with different origins of dispersal. The boundaries of the computational domain are at 75°N and 25°N, and 60°E and 15°W as shown in Figure 3, they are chosen to comfortably incorporate our pan-European area. The environmental factors included into the model are the altitude, latitude, coastlines and the Danube-Rhine river system. The equation describing the farming population also includes advection velocity $\mathbf{V}$ along the major waterways (the Danube, the Rhine and the sea coastlines; $\mathbf{V} \neq 0$ within corridors 10 km wide on each side of a river or 10 km inshore near the sea) which results from anisotropic diffusion in those areas. The prescription of the components of the advective velocity are given in Davison et al. (*2006*).

The focus of our model is the speed of the front propagation U, since this quantity can be most readily linked to the radiocarbon age used to date the 'first arrival' of the wave of advance. This feature of the solution depends only on the linear terms in Equation (2) and, in particular, is independent of the carrying capacity K. Moreover, to a first approximation U only depends on the product $\gamma\nu$:

$$U = 2\sqrt{\gamma\nu}. \qquad (3)$$

Taking the intrinsic growth rate of a farming population as $\gamma = 0.02$ year^{-1} (*Birdsell 1957*), the mean speed of the front propagation of $U \approx 1$ km/year for the population of farmers suggests the background (low-latitude) value of the diffusivity $\nu = 12.5$ km^2/year (*Ammerman and Cavalli-Sforza 1971; Davison et al. 2006*). For the wave spreading from Eastern Europe, $U \approx 1.6$ km/year is acceptable as a rough estimate obtained from the EE radiocarbon dates (*Dolukhanov et al. 2005*); this estimate is confirmed by our model (see Fig. 2d). Analysis of the spread of Paleolithic hunter-gatherers yields $U \approx 0.8$ km/year; the corresponding demographic parameters are suggested to be $\gamma = 0.02$–0.03 year^{-1} and $\nu = 50$–140 km^2/year (*Fort et al. 2004*). These authors use an expression for U different from Eq. (3); it is plausible, therefore, that the intrinsic growth rate obtained by Fort et al. (*2004*) for hunter-gatherers is a significant overestimate; for $\nu = 100$ km^2/year and $U \approx 1.6$ km/year, the nominal value of γ obtained from Eq. (3) is about 0.006 year^{-1}. A growth rate of $\gamma = 0.01$ year^{-1} has been suggested for indigenous North-American populations in historical times (*Young and Bettinger 1992*). The range $\gamma = 0.003$–0.03 year^{-1} is considered in a model of Paleoindian dispersal (*Steele et al. 1998*). Our simulations adopt $\gamma = 0.007$ year^{-1} and $\nu = 91.4$ km^2/year for the hunter-gatherers.

For the wave that spreads from the Near East carrying farming, K and ν smoothly tend to zero within 100 m of the altitude 1 km, above which land farming becomes impractical. For the wave spreading from the East, K and ν are similarly truncated at altitudes around 1500 km as foraging is possible up to higher altitude than farming. The low-altitude (background) values of K adopted are 0.07 persons/km^2 for hunter-gatherers (*Dolukhanov, 1979; Steele et al. 1998*) and 3.5 persons/km^2 for farmers, a value 50 times larger than that for hunter-gatherers (*Ammerman and Cavalli-Sforza 1984*). The values of K do not affect any results reported in this paper.

In seas, for both farmers and hunter-gatherers, both the intrinsic growth rate and the carrying capacity vanish as seas are incapable of supporting a human population. The diffusivity for both farmers and hunter gatherers tails off exponentially as

$$\nu \propto \exp(-d/l),$$

with d the shortest distance from the coast and $l = 40$ km, allowing the population to travel within a short distance offshore but not to have a sustained existence there. The value of l has been fine-tuned in this work in order to reproduce the delay, indicated by radiocarbon dates, in the spread of the Neolithic from the continent to Britain and Scandinavia. This provides an interesting inference regarding the sea-faring capabilities of the times, suggesting confident travel within about 40 km off the coast.

The inclusion of advection along the Danube-Rhine corridor and the sea coastlines is required to reproduce the spread of the Linear Pottery and Impressed Ware cultures obtained from the radiocarbon and archaeological evidence (see *Davison et al. 2006* for details). The speed of spread of farming in the Danube-Rhine corridor was as high as 4 km/yr (*Ammerman and Cavalli-Sforza 1971*) and that in the Mediterranean coastal areas was perhaps as high as 20 km/yr (*Zilhão 2001*); we set our advective velocity in these regions accordingly. However, there are no indications that similar acceleration could occur for the hunter-gatherers spreading from the East. Thus, we adopt $\mathbf{V} = 0$ for this population.

The starting positions and times for the two waves of advance – *i.e.*, the initial conditions – were selected as follows. For the population of farmers, we position the origin and adjust the starting time so as

to minimize the root mean square difference between the SCWE ^{14}C dates and the arrival time of the modelled population at the corresponding locations; the procedure is repeated for all positions between 30°N, 30°E and 40°N, 40°E with a 1° step. This places the centre at 35°N, 39°E, with the propagation starting at 6700 BC. For the source in the East of Europe, we have tentatively selected a region centered at 53°N, 56°E in the Ural mountains (to the east of the Neolithic sites used here), so that the propagation front reaches the sites in a well developed form. We do *not* suggest that pottery-making independently originated in this region. More reasonably, this technology spread, through the bottleneck between the Ural Mountains and the Caspian Sea, from a location further to the east. The starting time for this wave of advance was fixed by trial and error at 8200 BC at the above location; this reasonably fits most of the dates in Eastern Europe attributable to this centre. For both populations, the initial distribution of N is a truncated Gaussian of a radius 300 km.

Comparison of the model with radiocarbon dates

The quality of the model was assessed by considering the time lag $\Delta T = T - T_m$ between the modelled arrival time(s) of the wave(s) of advance to a site, T_m, and the actual ^{14}C date(s) of this site, T, obtained as described in Sect. 2. The sites were attributed to that centre (Near East or Urals) which provided the smallest magnitude of ΔT. This procedure admittedly favours the model, and the attributions have to be carefully compared with the archaeological and typological characteristics of each site. Such evidence is incomplete or insufficient in a great number of cases; we leave the laborious task of incorporating independent evidence in a systematic and de-

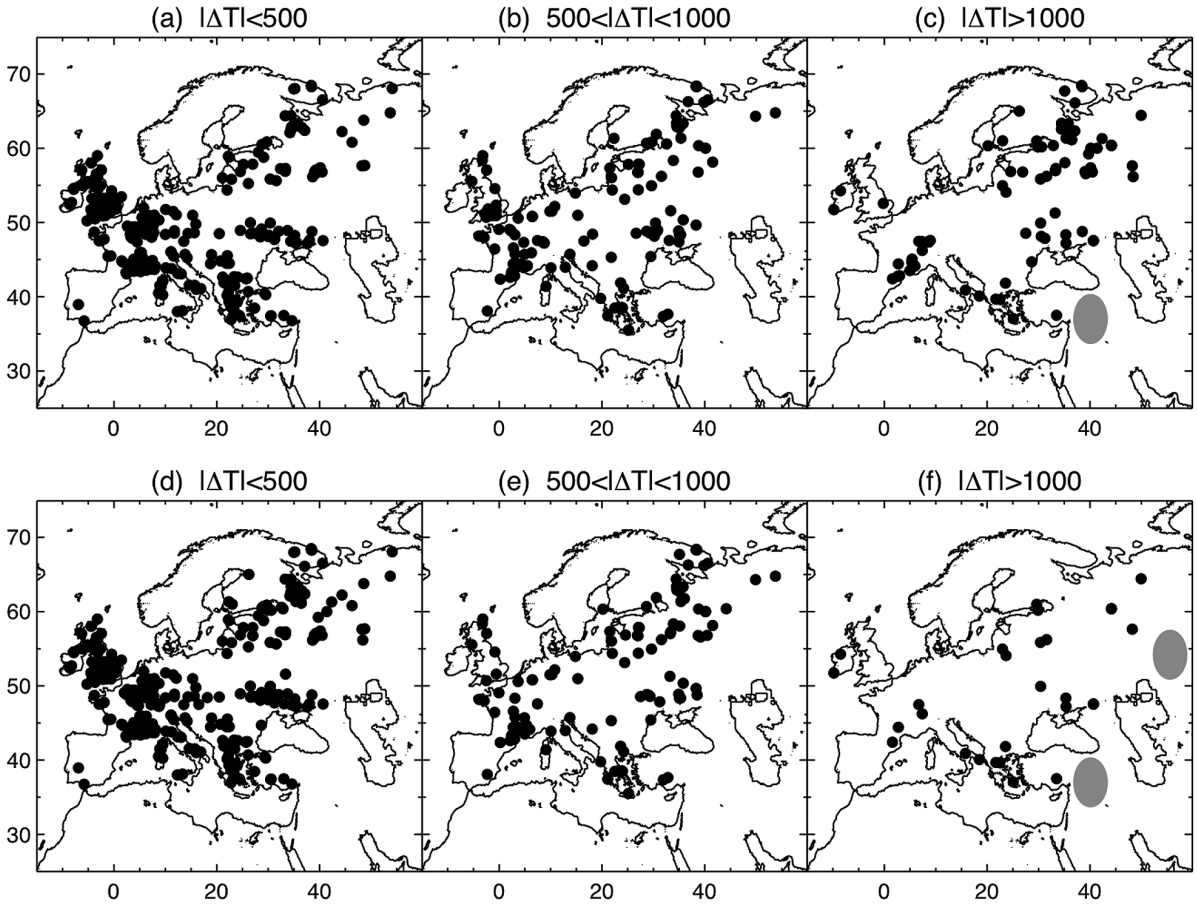

Fig. 3. Time lags, $\Delta T = T - T_m$, between the actual and modelled arrival times for the early Neolithic sites shown against their geographical position: panels (a)–(c) refer to a model with a single source in the Near East, and panels (d)–(f) to our best model with two sources (with the second on the Eastern edge of Europe). The positions of the sources are shown in grey in panels (c) and (f). Sites with $|\Delta T| < 500$ are shown in (a) and (d), those with 500 yr $< |\Delta T| <$ 1000 yr in panels (b) and (e), and those with $|\Delta T| >$ 1000 yr in panels (c) and (f). There are 265, 132, 80 sites in panels (a)–(c) and 336, 113, 28 sites in (d)–(f), respectively. Many data points corresponding to nearby sites overlap, diminishing the apparent difference between the two models. The advantage of the two-source model is nevertheless clear and significant.

tailed manner for future work. Our formulaic method of attribution has inevitably failed in some cases, but our preliminary checks have confirmed that the results are still broadly consistent with the evidence available, (see below).

First, we considered a model with a single source in the Near East (see Fig. 4a for histogram of time lags). The resulting time lags are presented in Figure 3a–c. The best fit model with two sources is similarly illustrated in Figure 3d–f. The locations of the two sources are shown with grey ellipses in panels (c) and (f).

In Figure 3a the sites shown are those at which the model arrival date and the radiocarbon date agree within 500 years (55 % of the pan-European dates); Figure 3d gives a similar figure for the two source model (now 70 % of the pan-European dates fit within 500 years). The points in the EE area are significantly more abundant in Figure 3d than in Figure 3a, while the difference in the SCWE area is less striking. The SCWE sites are better fitted with the one source model, with $|\Delta T| < 500$ years for 68 % of data points, but the fit is unacceptably poor for EE, where only 38 % of the radiocarbon dates can be fitted within 500 years. A convenient measure of the quality of the fit is the standard deviation of the time lags

$$s = \sqrt{\frac{1}{N}\sum_{i=1}^{N}\left(\Delta T_i - \overline{\Delta T}\right)} \quad \text{with} \quad \overline{\Delta T} = \frac{1}{N}\sum_{i=1}^{N}\Delta T_i .$$

The standard deviation of the pan-European time lags here is s = 800 years. Outliers are numerous when all of the European sites are included (illustrated by the abundance of points in Figure 3c), and they make the distribution skewed, and offset from $\Delta T = 0$ (see Fig. 4a). The outliers are mainly located in the east: for the SCWE sites, the distribution is more tightly clustered (s = 540 years), has negligible mean value, and is quite symmetric. In contrast, the time lags for sites in Eastern Europe (EE), with respect to the centre in the Near East, have a rather flat distribution (s = 1040 years), which is strongly skewed and has a significant mean value (310 years).

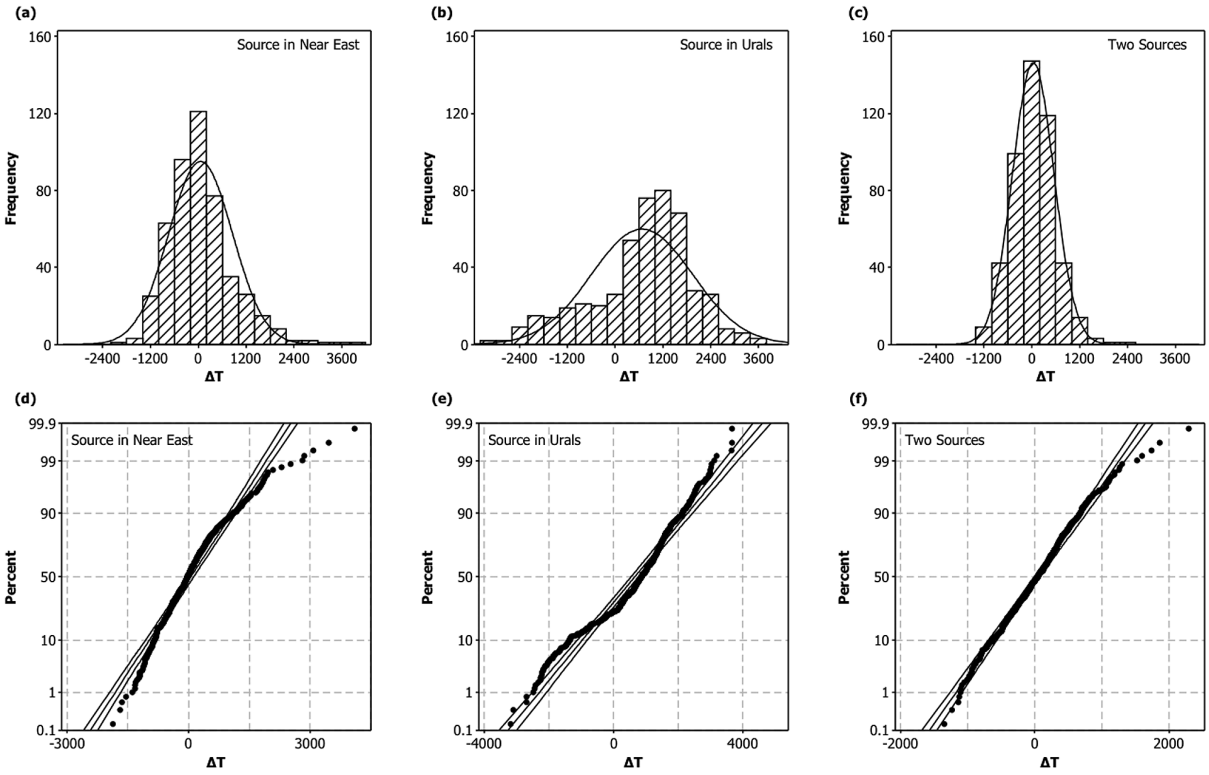

Fig. 4. Time lags, $\Delta T = T - T_m$, between the actual and modelled arrival times for the early Neolithic sites. (a)–(c): Histograms of the time lags, with a normal distribution fit (solid), for a model with a single source in the Near East (a), for a single source in the Urals (b) and for a two-source model (c). (d)–(f): The cumulative probability distribution of the time lags from panels (a)–(c), respectively, rescaled such that a normal probability distribution corresponds to a straight line (known as a normal probability plot). The straight lines show the best-fitting normal distribution, and the 95 % confidence interval. A significant reduction in the number of outliers can be seen in (f) or (c) as compared to (d) or (a) and (e) or (b). The distributions of panels (d) and (e) fail the Anderson-Darling normality test, while (f) passes the test confirming that ΔT is normally distributed (p-value = 0.149).

The failure of the single-source model to accommodate the ^{14}C dates from Eastern Europe justifies our use of a more complicated model that has two sources of propagation. Attempts were made at locating the single source in various other locations, such as the Urals, but this did not improve the agreement (see Fig. 4b for the histogram of time lags for the model with single source in the Urals).

Adding another source in the East makes the model much more successful: the values of the time lag, shown in Fig. 3d–f, are systematically smaller; *i.e.* there are significantly fewer points in Fig. 3f (5 %) compared to Fig. 3c (17 %). The resulting ΔT distribution for all the sites is quite narrow (s = 520 years) and almost perfectly symmetric, with a negligible mean value (40 years), see Fig. 4c. The distributions remain similarly acceptable when calculated separately for each source (with s = 490 and 570 years for the sites attributable to the Near East and Urals, respectively). The improvement is especially striking in EE, where the sites are split almost equally between the two sources.

We tentatively consider a model acceptable if the standard deviation, s, of the time lag ΔT is not larger than 3 standard dating errors σ, *i.e.*, about 500 years, given our estimate of σ close to 160 years over the pan-European domain. This criterion cannot be satisfied with any single-source model, but is satisfied with two sources. While we would never expect a large-scale model of the sort proposed here to accurately describe the complex process of the Neolithization in fine detail (and so the resulting values of ΔT cannot be uniformly small), the degree of improvement in terms of the standard deviation of ΔT clearly favours the two-source model. The reduction in s is statistically significant, and cannot be explained by the increase in the complexity of the model alone. The confidence intervals of the sample standard deviations s for one-source and two-source models do not overlap ($740 < \sigma < 840$ and $480 < \sigma < 550$, respectively); the F-test confirms the statistical significance of the reduction at a 99 % level.

It is also instructive to perform some further basic statistical analysis of the time lags ΔT. We use the Anderson-Darling test to assess if the sample of time lags can be approximated by the Gaussian probability distribution (*i.e.*, in particular, have a symmetric distribution with an acceptably small number of outliers). The null hypothesis of the test is that the time lags have a Gaussian distribution with the sample mean and standard deviation, while the alternative hypothesis is that they do not. This test leads us to accept the null hypothesis in the case of the two-source model (p-value = 0.149) while rejecting the null hypothesis for both one source models. Figure 4d–f show the cumulative probability distributions of the time lags for each model studied, rescaled such that a normal probability distribution corresponds to a straight line (known as a normal probability plot). The straight lines show the best-fitting normal distribution together with its 95 % confidence interval. As quantified by the test, the time lags more closely follow the straight line in (f) than in (d) or (e); the number of outliers is reduced very significantly in (f). Table 1 shows those sites that have $|\Delta T| >$ 1000 years, *i.e.*, where the disagreement between the data and the best-fit, two-source model is the strongest. There are 28 such sites: 14 of these have not undergone any statistical treatment, while the remaining 14 are a result of date combination or selection as described in Section 2. Five of the dates in Table 1 arise from the four sites (Berezovaya, Osipovka, Rakushechnyi Yar and Yerpin Pudas) where we have been unable to isolate less than three representative dates (see Section 2). This may suggest that a reinvestigation of these sites in particular is required and improved stratigraphic and typological data are required for these sites.

As further quantification of the quality of the model, the χ^2 statistic has been calculated for each model:

$$X^2 = \sum_{i=1}^{N} \frac{\left(\Delta T_i\right)^2}{\sigma_i^2}. \qquad (4)$$

The results are shown in Table 2.

The values of X^2, given in Table 2, may then be compared to the χ^2 value at the 5 % level with N–1 degrees of freedom (χ^2_{N-1} = 527.86). On all occasions the value of X^2 significantly exceeds χ^2_{N-1} (at 5 % level) this is not surprising given the simplicity of our model. The χ^2 statistical test would be satisfied if we discard about one third of the sites. It should be highlighted however that there is an approximate threefold increase in the accuracy of the model with two sources with respect to a single-source model. Some increase in the fit would be expected since we have increased the complexity of the model, but an increase of this magnitude surpasses what we believe could be attributed simply to the increase in model complexity. Development and application of further statistically robust techniques for comparison of our model with archaeological evidence is subject to our ongoing study.

				Sample				Site			Model arrival time	
Site Name	**Lab Index**	**Latitude deg.**	**Longitude deg.**	**Age BP yr**	**Error**	**Age cal BC yr**	**Calibration Error**	**Age cal BC yr**	**Calibration Error**	**Note**	**From Near East, yr BC**	**From Urals, yr BC**
Argisa Magula	UCLA-1657A	39.64	22.47	8130	100	7100	400	7100	400	One date	6052	3975
Balma Margineda	Ly-2439	42.41	1.58	6670	85	5600	130	5600	130	One date	6700	3256
Bavans	LV-1415	47.47	6.70	7130	70	6000	170	6000	170	One date	4903	3777
Berezovaya	LE-6706a	60.38	44.17	7840	75	6775	92	6775	92	Older date	3697	5509
Berezovaya	LE-67066	60.38	44.17	8700	300	7800	267	7800	267	Oldest date	3697	5509
Bolshoe Zavetnoye	LE-6556	60.98	29.63	7750	180	6650	150	6650	150	Oldest date	3836	4913
Canhasan III	BM-1666R	37.50	33.50	8460	150	7450	133	7338	233	Chi-Squared	5814	3664
Canhasan III	BM-1664R			8470	140	7450	133					
Canhasan III	BM-1660R			8390	140	7375	108					
Canhasan III	BM-1667R			8480	110	7450	100					
Canhasan III	BM-1662R			8460	110	7450	100					
Canhasan III	BM-1663R			8350	210	7300	233					
Canhasan III	BM-1665R			8270	160	7200	133					
Canhasan III	BM-1656R			8090	170	7050	150					
Canhasan III	HU-12			8543	66	7600	40					
Canhasan III	BM-1658R			8060	130	7025	142					
Canhasan III	HU-11			8584	65	7635	38					
Canhasan III	BM-1657R			8080	130	7050	133					
Carrowmore	Lu-1840	54.27	-8.53	5750	85	4575	215	4575	215	One date	3517	2445
Cashelkeelty	UB-2413	51.72	-9.82	5845	100	4695	245	4695	245	One date	3585	2267
Choinovtyi-1	LE-5164	64.42	49.95	4640	25	3435	28	4070	595	Average of site one	2963	5374
Choinovtyi-1	LE-1729			5320	60	4160	57					
Choinovtyi-1	LE-4495			5750	70	4615	55					
DobriniöĔe	Bln-3785	41.83	23.57	6650	60	5575	32	5575	32	One date	6700	4199
Dubokrai-5	Le-3003	55.85	30.37	4720	40	3505	45	3578	160	Average of middle peak	4628	5025
Dubokrai-6	Le-6279			4820	130	3650	117					
Golubjai-1	LE-4714	54.95	22.98	7060	270	5950	167	5950	167	Older date	4577	4703
Grotta del Sant	R-284	40.90	15.78	5555	75	4395	155	4395	155	One date	5722	3326
della Madonna												
Grotta di Porto Badisco	R-1225	40.08	18.48	5850	55	4675	135	4675	135	One date	5815	3452
Kamennaya Mogila	Ki-4023	47.20	35.35	5120	80	3975	92	3975	92	Younger date	5675	4984
Koshinskaya	LE-6629	57.63	48.23	8350	100	7360	73	7360	73	Older date	3896	5767
Kurkijokki	LE-6929	60.18	29.88	7900	80	6825	75	6825	75	One date	3973	4963
Marevka	OxA-6199	48.35	35.30	7955	55	6865	62	6865	62	Older date	5566	5042
Osipovka	OxA-6168	49.93	30.40	7675	70	6535	38	6535	38	Older date	5473	4896
Planta	CRG-280	46.23	7.37	6500	80	5465	155	5465	155	One date	6700	3697
Racquemissou VIII c1		44.42	2.73	7400	300	6400	233	6400	233	One date	5209	3445
Rakushechnyi Yar	Le-5387	47.55	40.67	4830	90	3585	72	3862	283	Average of younger cluster	5417	5209
Rakushechnyi Yar	Le-5340			5060	230	3850	183					
Rakushechnyi Yar	Le-5327			5290	260	4150	217					
Rakushechnyi Yar	Le-5344	47.55	40.67	7180	250	6050	167	6600	319	Average from older cluster	5417	5209
Rakushechnyi Yar	Ki-6475			7690	100	6600	83					
Rakushechnyi Yar	Ki-955			7840	105	6750	100					
Rakushechnyi Yar	Ki-6477			7860	130	6775	108					
Rakushechnyi Yar	Ki-6476			7930	140	6825	125					
Saliagos	P-1311	37.05	25.08	6172	74	5080	230	5080	230	One date	6165	3471
Serteya-10	Le-5260	56.22	31.57	7350	180	6200	133	6225	317	Average of older dates	4571	5081
Serteya-10	Le-5261			7300	400	6250	317					
Theopetra Cave	DEM.576	39.68	21.68	8060	32	6980	53	6980	53	One date	5969	3980
Zapes	Vs-977	54.08	23.67	4860	260	3600	233	3600	233	One date	4708	4716

It is instructive to represent the data in the same format as in Figure 2a, b, but now with each date attributed to one of the sources, as suggested by our model. This has been done in Figure 2c, d, where the close correlation of Figure 2a is restored for the pan-European data. Now, the dates are consistent with constant rates of spread from one of the two sources. Using straight-line fitting, we obtain the average speed of the front propagation of 1.1 ± 0.1 km/year for the wave originating in the Near East (Fig. 2c), and 1.7 ± 0.3 km/year for the source in the East (Fig. 2d); 2σ values are given as uncertainties here and below. The spread from the Near East slowed down in Eastern Europe to 0.7 ± 0.1 km/year; the dates from the west alone (as in Fig. 2a) gives a higher speed of 1.2 ± 0.1 km/year. The estimates for the data in both western and eastern Europe are compatible with earlier results (*Dolukhanov et al. 2005; Gkiasta et al. 2003; Pinhasi et al. 2005*). Care must be taken when using such estimates, however, since the spread occurs in a strongly heterogeneous space, and so cannot be fully characterised by a single constant speed. The rate of spread varies on both pan-European scale and on smaller scales, *e.g.*, near major waterways (*Davison et al. 2006*).

Our allocation of sites to sources suggested and used above requires careful verification using independent evidence. Here we briefly discuss a few sites. Taking Ivanovskoye-2 (56.85°N, 39.03°E) as an example, the data form two peaks (Fig. 1b); the times at which each of the waves arrive at this location are 4349 BC (for the Near-Eastern wave) and 5400 BC (for the Eastern wave) closely fitting the two peaks in ^{14}C dates. As another example, we accept two dates for the Mayak site (68.45°N, 38.37°E); one from the younger cluster (2601 ± 192 BC), and also the older date (4590 ± 47 BC) detached from the cluster. The younger cluster is consistent with the near-eastern wave (arriving at 2506 BC) and the older date with the Eastern wave (arriving at 4718 BC).

Tab. 1 (on previous page). The 28 sites where the deviation of the model arrival times from the ^{14}C dates exceeds 1000 years, $|\Delta T| > 1000$ years: (1) site name; (2) laboratory index; geographical (3) latitude and (4) longitude in degrees; (5) uncalibrated age and (6) its 1σ laboratory error in years (BP); (7) calibrated age and (8) its 1 σ error in years (BC); (9) combined site calibrated age and (10) its 1σ error in years (BC) obtained as discussed in Section 2; (11) method used to select this date; and the model arrival times (years BC) for the wave spreading from (12) the Near East and (13) the Urals. The data are presented in alphabetical site name order.

Model	X^2
Single source in Near-East	9553
Single source in Urals	28268
Two-source model	3740

Tab. 2. The X^2 test statistic, given by Eq. (4), for each model.

We further consider those sites which are geographically in the west (*i.e.*, to the west of a boundary set to join the Baltic Sea to the Black Sea) but are allocated to the source of pottery making in the Ural mountain area. These sites are shown in Table 3. There are 40 such sites (*i.e.*, 14 % of sites in the west); they deserve further analysis in order to verify the attribution suggested by the model and, if necessary, to further refine the model to improve the agreement with the archaeological data. There are also 104 sites in the east of the above boundary that are allocated to the source of farming in the Near East (*i.e.* 56 % of data points in the east). These sites are listed in Table 4. Where a site is characterised by a combined date obtained as described above, only the final age estimate is given (see entry in the column labelled 'Note' for the selection technique applied). All sites in Tables 3 and 4 should be reassessed both in terms of the statistical processing of multiple measurements and in terms of the agreement with independent archaeological data.

Conclusions

Our model has significant implications for the understanding of the Neolithization of Europe. It substantiates our suggestion that the spread of the Neolithic involved at least two waves propagating from distinct centres, starting at about 8200 BC in Eastern Europe and 6700 BC in the Near East. The earlier wave, spreading from the east via the 'steppe corridor', resulted in the establishment of the 'eastern version' of the Neolithic in Europe. A later wave, originating in the Fertile Crescent of the Near East, is the better-studied process that brought farming to Europe.

It is conceivable that the westernmost extension of the earlier (eastern) wave of advance produced the pre-agricultural ceramic sites of La Hoguette type in north-eastern France and western Germany, and Roucadour-type (also known as Epicardial) sites in western Mediterranean and Atlantic France (*Berg and Hauzer 2001; Jeunesse 1987*). The available dates for the earlier Roucadour sites (7500–6500 BC) (*Roussault-Laroque 1990*) are not inconsistent with

				Sample				Model arrival time	
Site Name	Lab index	Latitude deg.	Longitude deg.	Age BP, yr	Error	Age cal BC, yr	Calibration Error	From Near East, yr BC	From Urals, yr BC
Abri de la Coma Franceze	Gif-9080	42.83	2.92	5180	60	4010	220	5338	3327
Bridgemere	BM-2565	51.21	-2.41	4630	50	3375	275	4291	3156
Burntwood Farm. R6	OxA-1384	51.12	-1.29	4750	50	3510	140	4324	3232
Bury Hill		50.92	-1.37	4750	50	3510	140	4343	3223
Chatelliers du Viel	Gif-5717	46.43	-0.87	5200	110	4025	325	4829	3402
Cherhill	BM-493	51.43	-1.95	4715	90	3400	300	4276	3186
Coma Franceze	Gif-7292	42.83	2.92	5200	70	4025	225	5338	3327
Corhampton	BM-1889	50.98	-1.15	4790	70	3535	165	4334	3237
Coufin	Ly-3321	45.07	5.40	5260	120	4050	300	5188	3565
Derriere les Pres	WM	49.07	-0.05	5110	70	4030	320	4576	3502
Feldbach	UCLA-1809A	47.23	8.78	5170	70	4010	220	4998	3861
Fendmeilen	UCLA-1691F	47.28	8.63	5415	60	4200	160	4998	3857
Fengate	GaK-4196	52.57	-0.21	4960	64	3145	225	4198	3200
Frankenau	VRI-207	47.50	16.50	5660	100	4525	125	5377	4213
Frigouras	GIF-8479	44.13	5.95	5450	100	4250	210	5341	3506
Grande Louvre	GIF-7618	48.87	2.33	5260	70	4105	155	4612	3619
Greifensee	WM	47.37	8.68	5140	49	3920	130	5010	3861
Grotta dei Ciclami	WM	45.70	4.92	5445	60	4245	205	5114	3597
Grotta del Sant della Madonna	R-284	40.90	15.78	5555	75	4395	155	5722	3326
Grotte de la Vieille Eglise	WM	45.92	6.28	5295	52	4115	135	5018	3657
Grotte du Sanglier	WM	44.68	5.33	5440	130	4250	300	5268	3531
Honeygore Track	GaK-1939	51.18	-2.82	4590	40	3305	205	4298	3130
Horné Lefantovce	Bln-304	48.42	18.17	5775	140	4700	200	5396	4318
Le Coq Galleux	WM	49.40	2.73	5300	140	4100	350	4554	3652
Le Trou du Diable	Ly-6505	47.32	4.78	5105	55	3905	135	4870	3682
Les Coudoumines	WM	42.75	2.57	5135	36	3920	120	5309	3315
Les Longrais	Ly-150	46.58	2.77	5290	150	4100	167	4898	3561
Mannlefelsen	Gif-2634	47.45	7.23	5140	140	3950	300	4954	3800
Millbarrow	OxA-3172	51.45	-1.87	4900	110	3675	325	4277	3191
Peak Camp	OxA-1622	51.83	-2.15	4865	80	3650	300	4224	3163
Phyn	WM	47.58	8.93	4993	28	3820	120	5029	3883
Redlands Farm	OxA-5632	52.33	-0.59	4825	65	3545	165	4209	3211
Sente Saillancourt	Gif-5840	49.08	2.00	5220	110	4050	300	4569	3609
Shurton Hill	UB-2122	50.92	-0.58	4750	50	3510	140	4346	3282
Source de Reselauze	WM	43.52	4.98	5380	110	4210	240	5424	3460
Windmill Hill	OxA-2395	50.92	-1.88	4730	80	3505	155	4335	3183
Winnall Down	HAR-2196	51.08	-1.32	4800	80	3540	180	4324	3226
Zurich	UCLA-1772B	47.37	8.58	5145	70	3975	275	5010	3857
Zurich-Bauschanze	WM	47.41	8.52	5320	60	4155	175	5018	3857
Zurich-Wollishofen	WM	47.41	8.52	4993	46	3805	145	5018	3857

Tab. 3. The 40 sites which are allocated to the source of spread in the Urals but are located to the west of a west-east borderline joining the Baltic Sea to the Black Sea: (1) site name; (2) laboratory index; geographical (3) latitude and (4) longitude in degrees; (5) uncalibrated age and (6) it's 1σ laboratory error in years (BP); (7) calibrated age and (8) it's 1σ error in years (BC); and the model arrival times (years BC) for the wave spreading from (9) the Near East and (10) the Urals. The data are presented in alphabetical site name order.

			Site			Model arrival time	
Site Name	**Latitude deg.**	**Longitude deg.**	**Age cal BC, yr**	**Calibration Error**	**Note**	**From Near East, yr BC**	**From Urals, yr BC**
Babshin	48.47	26.57	5160	50	One date	5518	4680
Bara	60.00	40.15	2900	150	One date	3884	5386
Bazkov Isle	48.08	28.47	5568	160	Average of the younger cluster	5660	4745
Bazkov Isle	48.08	28.47	6143	160	Average of the older cluster	5660	4745
Berendeevo-2a	56.57	39.17	3883	187	Average of middle peak	4376	5408
Bernashovka	48.55	27.50	5565	212	Average of older cluster	5552	4722
Besovy Sledki	64.38	34.43	3190	60	Younger date	3310	4993
Besovy Sledki	64.38	34.43	4010	205	Average of older three dates	3310	4993
Bilshivtsy	48.93	24.58	5307	160	Average	5353	4610
Chapaevka	47.30	35.52	5853	160	Average	5663	5000
Chernaya Guba-4	62.82	34.87	3414	316	Average of younger cluster	3558	5104
Chernushka-1	57.68	48.77	3995	276	Average	3875	5784
Choinovtyi -2	64.30	49.87	3668	11	One date	2977	5379
Choinovtyi-1	64.42	49.95	4070	595	Average of site one	2963	5374
Daktariske	55.82	22.87	4350	100	Oldest date	4454	4707
Drozdovka	68.33	38.28	1535	52	One date	2510	4716
Dubokrai-5	55.85	30.37	3578	160	Average of middle peak	4628	5025
Dubokrai-5	55.85	30.37	4700	600	Oldest Date	4628	5025
Gard-3	47.70	31.20	5722	160	Average	5800	4839
Ivanovskoye-2	56.85	39.03	4094	201	Weighted average of younger peak. X^2	4349	5400
Kääpa	57.87	27.10	3509	217	Average of older cluster	4299	4898
Kamennaya Mogila	47.20	35.35	5717	460	Average of older cluster	5675	4984
Kizilevyj-5	48.25	35.15	5640	53	One date	5580	5031
Kodrukõla	59.45	28.08	3590	160	Average	4081	4929
Korman	48.57	27.23	5193	160	Average	5541	4712
Koshinskaya	57.63	48.23	3550	167	Younger Date	3896	5767
Krivina-3	54.95	29.63	4145	58	Older date	4755	4986
Krivun	68.28	38.43	2685	65	Younger date	2518	4726
Krivun	68.28	38.43	3375	92	Older date	2518	4726
Kuzomen	66.27	36.77	2100	200	One date	2733	4791
Lanino-2	57.18	33.00	4779	533	Average of older cluster	4431	5144
Lasta -8	64.77	53.73	2690	70	One date	2780	5381
Lasta -8	64.77	53.73	3500	267	One date	2780	5381
Maieri-2	61.88	30.57	2975	125	One Date	3657	4971
Mamai Gora	47.47	34.38	5940	160	Average	5664	4964
Marevka	48.35	35.30	6477	167	Average	5566	5042
Marevka	48.35	35.30	6865	62	One date	5566	5042
Mariupol Cemetry	47.15	37.57	5518	160	Average	5636	5075
Marmuginsky	60.80	46.30	3500	47	One date	3564	5554
Mayak	68.45	38.37	2601	192	Weighted average. X^2	2506	4718
Modlona	60.35	38.80	3067	575	Average	3873	5327
Mys-7	67.98	34.97	2660	63	Older date	2665	4685
Navolok	66.50	40.58	2975	125	Younger date	2777	4922
Navolok	66.50	40.58	3575	68	Older date	2777	4922
Nerpichya Guba	68.37	38.38	2275	108	Younger date	2506	4718
Nerpichya Guba	68.37	38.38	3325	108	Older date	2506	4718
Okopy	49.97	26.53	5458	223	Average	5334	4730
Orovnavolok	62.77	35.08	2790	33	One date	3570	5116
Ortinokh-2	68.05	54.13	2035	55	One date	2317	5132
Osa	56.85	24.58	4434	435	Average of middle cluster	4380	4795
Oshchoy - 2	63.77	48.58	3230	47	One date	3099	5406
Osipovka	49.93	30.40	6535	38	One Date	5473	4896
Osipovsky Liman	48.87	34.92	6400	57	One date	5514	5047
Pechora	48.83	28.70	6117	160	Average	5573	4782

Pegrema-3	62.58	34.43	3433	506	Average of younger cluster	3598	5099
Pleshcheyevo-3	56.78	38.70	3505	45	Oldest date	4371	5386
Povenchanko-15	62.82	34.85	2875	72	One date	3558	5104
Pugach-2	47.85	31.23	5633	160	Average of older cluster	5780	4850
Pyalitsa-18	66.18	39.83	3500	47	One date	2823	4945
Rakushechnyi Yar	47.55	40.67	5456	333	Average from middle cluster	5417	5209
Rakushechnyi Yar	47.55	40.67	6600	319	Average from older cluster	5417	5209
Razdolnoye	47.60	38.03	5475	160	Average	5571	5112
Repishche	58.35	33.88	3313	160	One Date	4252	5176
Rudnya Serteyskaya	55.63	31.57	4381	233	Chi-Squared	4656	5077
Sakhtysh-8	56.80	40.47	4068	189	Weighted average	4296	5465
Sarnate	57.33	21.53	3290	233	Average	4201	4639
Savran	48.12	30.02	5853	160	Average	5720	4808
Semenovka	48.28	30.13	5863	262	Average	5702	4822
Semenovka-5	45.42	29.50	5455	179	Average	5979	4615
Serteya-10	56.22	31.57	3688	200	Ave of young dates (exc. Corded)	4571	5081
Sev. Salma	68.03	35.18	3050	483	One date	2661	4687
Sheltozero-10	61.35	35.35	3000	117	Youngest date	3791	5173
Silino	60.85	29.73	3820	160	Average of younger cluster	3865	4919
Skibinsky	48.57	29.35	6303	160	Average	5631	4801
Sokoltsy-2	48.72	29.12	6253	160	Average	5600	4796
Spiginas	56.02	21.85	3850	167	Older date	4393	4670
Sukhaya Vodla-2	62.40	37.10	3540	57	One date	3604	5194
Sulka	56.75	27.00	3890	346	Average of middle cluster	4452	4891
Suna-12	62.10	34.22	4005	75	One Date	3677	5108
Surskoi Isle	48.32	35.07	6110	160	Average	5570	5032
Šventoji 9	56.02	21.08	3950	100	Oldest date	4354	4653
Syaberskoye-3	58.78	29.10	3750	217	Older date	4193	4975
Tamula	57.85	26.98	4150	60	Oldest date	4298	4894
Tekhanovo	57.07	39.28	4100	47	One date	4308	5409
Tokarevo	60.50	28.77	3450	183	One date	3883	4904
Tugunda-14	64.37	33.30	2848	160	Average	3324	4974
Vashutinskaya	57.37	40.13	3835	45	Yougest date	4243	5445
Vodysh	58.13	41.53	3275	125	One date	4087	5487
Voynavolok-24	62.90	34.57	2838	160	Average of younger cluster	3546	5092
Voynavolok-24	62.90	34.57	3115	72	Older date	3546	5092
Vozhmarikha -4	63.33	35.78	3620	160	Average of younger cluster	3477	5113
Vyborg	60.67	28.65	3260	80	One date	3855	4893
Yazykovo-1a	57.27	33.37	4700	177	Chi Squared	4416	5157
Yerpin Pudas	63.35	34.48	4175	160	Average of yougest cluster	3482	5072
Yumizh-1	62.23	44.35	3000	221	Average	3446	5416
Zalavruga-4	62.80	36.47	3333	286	Average of older cluster	3547	5159
Zapes	54.08	23.67	3600	233	One date	4708	4716
Zarachje	56.15	38.63	4515	52	One date	4448	5387
Zatsen'ye	54.40	27.07	4255	68	One date	4778	4868
Zedmar-D	54.37	22.00	3898	250	Weighted average. X^2	4607	4651
Zejmatiške	55.25	26.15	4355	38	Oldest date	4640	4841
Zolotets-6	62.78	36.53	3688	442	Average of older cluster	3560	5162
Zveisalas	57.83	27.25	3730	70	One date	4302	4904
Zvejnieki	57.82	25.17	4211	273	Average of younger cluster	4257	4824

Tab. 4 (beginning on previous page). The 104 sites which are allocated to the source of spread in the Near East but are located to the east of a west-east borderline joining the Baltic Sea to the Black Sea: (1) site name; geographical (2) latitude and (3) longitude in degrees; (4) calibrated age and (5) its 1σ error in years (BC); (6) method used to select this date; and the model arrival times (years BC) for the wave spreading from (7) the Near East and (8) the Urals. For sites with multiple ^{14}C dates only one (or a few) representative dates are given, obtained as discussed in Section 2. The selection method applied is given in the column labelled Note. The data are presented in alphabetical site name order.

this idea, but a definitive conclusion needs additional work.

The nature of the eastern source needs to be further explored. The early-pottery sites of the Yelshanian Culture (*Mamonov 2000*) have been identified in a vast steppe area stretching between the Lower Volga and the Ural Rivers. The oldest dates from that area are about 8000 BC (although the peak of the culture occurred 1000 years later) (*Dolukhanov et al. 2005*). Even earlier dates have been obtained for pottery bearing sites in Southern Siberia and the Russian Far East (*Kuzmin and Orlova 2000; Timofeev et al. 2004*). This empirical relation between our virtual eastern source and the earlier pottery-bearing sites further east may indicate some causal relationship.

According to our model, the early Neolithic sites in Eastern Europe belong to both waves in roughly equal numbers (56 % to near-eastern wave and 44 % to eastern wave). Unlike elsewhere in Europe, the wave attributable to the Near East does not seem to have introduced farming in the East. The reason for this is not clear and may involve the local environment where low fertility of soils and prolonged winters are combined with the richness of aquatic and terrestrial wildlife resources (*Dolukhanov 1996*).

Regardless of the precise nature of the eastern source, the current work suggests the existence of a wave which spread into Europe from the east carrying the tradition of early Neolithic pottery-making. If confirmed by further evidence (in particular, archaeological, typological, and genetic), this suggestion will require serious re-evaluation of the origins of the Neolithic in Europe.

ACKNOWLEDGEMENTS

Financial support from the European Community's Sixth Framework Programme under the grant NEST–028192–FEPRE is acknowledged.

∴

REFERENCES

AMMERMAN A. J. & BIAGI P. (eds.), 2003. *The Widening Harvest. The Neolithic Transition in Europe: Looking Back, Looking Forward*. Archaeological Institute of America. Boston.

AMMERMAN A. J. & CAVALLI-SFORZA L. L. 1971. Measuring the rate of spread of early farming in Europe. *Man 6: 674–688*.

1973. A Population Model for the Diffusion of Early Farming in Europe. In C. Renfrew (ed.), *The Explanation of Culture Change; Models in Prehistory*. London, Duckworth.

1984. *The Neolithic Transition and the Genetics of Populations in Europe*. Princeton University Press. Princeton.

BERG P. L. V. & HAUZER A. 2001. Le Néolithique ancien. *Anthropologica et Praehistoria 112: 63–76*.

BIRDSELL J. B. 1957. Some population problems involving Pleistocene man. *Cold Spring Harbor Symposium on Quantitative Biology 22: 47–69*.

BRONK RAMSEY C. 2001. Development of the Radiocarbon Program OxCal. *Radiocarbon 43: 355–363*.

CAVALLI-SFORZA L. L. & FELDMAN M. W. 1981. *Cultural Transmission and Evolution: A Quantitative Approach*. Princeton University Press. Princeton.

DAVISON K., DOLUKHANOV P. M., SARSON G. R. & SHUKUROV A. 2006. The role of waterways in the spread of the Neolithic. *Journal of Archaeological Science 33: 641–652*.

DOLUKHANOV P. 1979. *Ecology and Economy in Neolithic Eastern Europe*. Duckworth. London.

DOLUKHANOV P., SHUKUROV A., GRONENBORN D., SOKOLOFF D., TIMOFEEV V. & ZAITSEVA G. 2005. The Chronology of Neolithic Dispersal in Central and Eastern Europe. *Journal of Archaeological Science 32: 1441–1458*.

DOLUKHANOV P. M. 1996. *The Early Slavs: Eastern Europe from the Initial Settlement to the Kievan Rus*. Longman.

FORT J., PUJOL T. & CAVALLI-SFORZA L. L. 2004. Palaeolithic populations and waves of advance. *Cambridge Archaeological Journal 14: 53–61*.

GKIASTA M., RUSSELL T., SHENNAN S. & STEELE J. 2003. Neolithic transition in Europe: the radiocarbon record revisited. *Antiquity 77: 45–61*.

GORDON CHILDE V. 1925. *The Dawn of European civilization*. Kegan Paul, Trench & Trubner. London.

HAAK W., FORSTER P., BRAMANTI B., MATSUMURA S., BRANDT G., TÄNZER M., VILLEMS R., RENFREW C., GRONENBORN D., ALT K. W. & BURGER J. 2005. Ancient DNA from the first European farmers in 7500-year-old Neolithic sites. *Science 310: 1016–1018*.

JEUNESSE C. 1987. *Le céramique de la Hauguette. Un nouvel élément non rubané du Néolithique ancien de l'Europe de nord-ouest*. Cahiers Alsasiens.

KUZMIN Y. V. & ORLOVA L. 2000. The Neolithization of Siberia and the Russian Far East: Radiocarbon evidence. *Antiquity 74: 356–364*.

LUBBOCK J. 1865. *Pre-historic Times: as Illustrated by Ancient Remains, and the Manners and Customs of Modern Savages*. Williams and Norgate. London.

MAMONOV E. A. 2000. Khronologicheskii aspekt izucheniya yelshanskoi kul'tury. In E. N. Nosov (ed.), *Khronologiya Neolita Vostochnoi Evropy*. IIMK. St. Petersburg.

MURRAY J. D. 1993. *Mathematical Biology*. Springer-Verlag. Berlin.

OSHIBKINA S. V. 1996. Introduction. In S. V. Oshibkina (ed.), *Neolit Severnoi Evrazii*. Nauka. Moscow.

PERLÈS C. 2001. *The Early Neolithic in Greece. The First Farming Communities in Europe*. Cambridge University Press. Cambridge.

PINHASI R., FORT J. & AMMERMAN A. J. 2005. Tracing the Origin and Spread of Agriculture in Europe. *P.L.O.S. Biology 3: 2220–2228*.

PRICE T. D. 2000. *Europe's First Farmers*. Cambridge University Press. Cambridge.

ROUSSAULT-LAROQUE J. 1990. Rubané et Cardial, le poids de l'ouest. *Rubané et Cardial, ERAUL(Liège) 39: 315–360*.

SHENNAN S. & STEELE J. 2000. *Spatial and Chronological Patterns in the Neolithisation of Europe*. on-line: http://ads.ahds.ac.uk/catalogue/resources.html?c14_meso

STEELE J., ADAMS J. & SLUCKIN T. 1998. Modelling Paleoindian Dispersals. *World Archaeology 30: 286–305*.

THISSEN L., REINGRUBER A. & BISCHOFF D. 2006. *CANeW, ^{14}C databases and chronocharts (2005–2006 updates)*. on-line: http://www.canew.org/data.html

THOMAS J. 1996. The cultural context of the first use of domesticates in Continental and Northwest Europe. In D. R. Harris (ed.), *The Origins of Spread of Agriculture and Pastoralism in Eurasia*. UCL Press, London.

TILLEY C. 1994. *A Phenomenology of Landscape*. Berg. Oxford.

TIMOFEEV V. I., ZAITSEVA G. I., DOLUKHANOV P. M. & SHUKUROV A. M. 2004. *Radiocarbon Chronology of the Neolithic in Northern Eurasia*. Tesa. St. Petersburg.

WHITTLE A. 1996. *Europe in the Neolithic. The Creation of New Worlds*. Cambridge University Press. Cambridge.

YOUNG D. A. & BETTINGER R. L. 1992. The Numic Spread: A Computer Simulation. *American Antiquity 57: 85–99*.

ZILHÃO J. 2001. Radiocarbon evidence for maritime pioneer colonization at the origins of farming in west Mediterranean. *Proceedings of the National Academy of Sciences of the United States of America 98: 14180–14185*.

ZVELEBIL M. 1996. The agricultural frontier and the transition to farming in the circum-Baltic region. In D. R. Harris (ed.), *The Origins and Spread of Agriculture and Pastoralism in Eurasia*. UCL Press, London.